J Mater Sci: Mater Med (2009) 20:1159–1165
DOI 10.1007/s10856-008-3668-y

Proliferation and function of MC3T3-E1 cells on freeze-cast hydroxyapatite scaffolds with oriented pore architectures

Qiang Fu · Mohamed N. Rahaman · B. Sonny Bal · Roger F. Brown

Received: 7 September 2008 / Accepted: 15 December 2008 / Published online: 30 December 2008

Abstract Previous work by the authors showed that hydroxyapatite (HA) scaffolds with different types of oriented microstructures and a unique 'elastic–plastic' mechanical response could be prepared by unidirectional freezing of suspensions. The objective of the present work was to evaluate the in vitro cellular response to these freeze-cast HA scaffolds. Unidirectional scaffolds with approximately the same porosity (65–70%) but different pore architectures, described as 'lamellar' (pore width = 25 ± 5 μm) and 'cellular' (pore diameter = 100 ± 10 μm), were evaluated. Whereas both groups of scaffolds showed excellent ability to support the proliferation of MC3T3-E1 pre-osteoblastic cells on their surfaces, scaffolds with the cellular-type microstructure showed far better ability to support cell proliferation into the pores and cell function. These results indicate that freeze-cast HA scaffolds with the cellular-type microstructure have better potential for bone repair applications.

Q. Fu · M. N. Rahaman (✉)
Department of Materials Science and Engineering, Missouri University of Science and Technology, Rolla, MO 65409, USA
e-mail: rahaman@mst.edu

Q. Fu · M. N. Rahaman · R. F. Brown
Center for Bone and Tissue Repair and Regeneration, Missouri University of Science and Technology, Rolla, MO 65401, USA

B. S. Bal
Department of Orthopaedic Surgery, University of Missouri-Columbia, Columbia, MO 65212, USA

R. F. Brown
Department of Biological Sciences, Missouri University of Science and Technology, Rolla, MO 65409, USA

1 Introduction

Bioactive glass, glass-ceramics, and ceramics, such as 45S5 bioactive glass and hydroxyapatite (HA), referred to collectively as 'bioactive ceramics', are an important category of biomaterials that have promising potential for use in bone repair and regeneration [1–3]. Several methods have been used to produce porous scaffolds of bioactive ceramics, such as incorporation of a pore-producing fugitive phase such as starch or PVA [4, 5], the use of foaming agents [6, 7], polymer foam replication techniques [8–10], slip casting [11], and solid freeform fabrication [12, 13]. A limitation of scaffolds prepared by current methods is that they often lack the combination of high strength and high porosity for skeletal substitution of load-bearing bones. They are limited to low-stress applications instead, such as filling of contained bone defects, where adjacent, intact bone provides mechanical rigidity and support. The repair of large defects in load-bearing bones requires scaffolds with far higher strengths. Situations in which long bone discontinuity is encountered include traumatic injuries suffered in war or in automobile accidents, bone resection for tumors, and bone loss from complex, revision total hip or total knee surgery.

Recently, a method based on unidirectional freezing of aqueous suspensions has been shown to produce porous HA constructs with an oriented, lamellar-type microstructure and high compressive strength in the direction of orientation [14–18]. Compressive strengths as high as 65 MPa (56% porosity) in the direction parallel to the freezing direction were reported for testing of small HA disks [14, 15]. However, the pore width of these lamellar-type HA constructs was only 10–40 μm, a value that is considered too low for tissue ingrowth. A porosity of >50% with pore size (diameter or width) of 100 μm or

larger are the minimum values reported for scaffolds capable of supporting cell proliferation and function [19, 20].

Our previous work [16–18] using a unidirectional freezing method showed that the addition of polar organic solvents such as 1,4-dioxane (referred to simply as dioxane) and glycerol to aqueous suspensions of HA resulted in drastic changes to the microstructure. Compared to the lamellar-type microstructure (pore width 10–40 μm) obtained from aqueous suspensions, scaffolds with approximately the same porosity (65–70%) prepared from suspensions with 60 wt% dioxane had a cellular-type microstructure with nearly cylindrical pores of diameter 90–110 μm. When compared to the common brittle failure of ceramics, the deformation of the freeze-cast scaffolds in compression showed a unique 'elastic–plastic' response. The freeze-cast constructs were deformed to large strains (>20–50%) without disintegrating in a brittle manner.

Based on the unique mechanical response and the favorable pore characteristics of the HA constructs with the cellular-type microstructure [17], this in vitro investigation was undertaken to evaluate the ability of these oriented constructs to support cell proliferation and function. For comparison, the in vitro cellular response to the lamellar-type constructs was also studied. The mouse MC3T3-E1 cell line chosen for this study is a well-characterized pre-osteoblastic cell line that has been used extensively in previous in vitro investigations of biomaterials for bone repair and tissue engineering [21, 22].

2 Materials and methods

2.1 Preparation of HA scaffolds

Methods for preparing HA scaffolds with an oriented microstructure by unidirectional freezing of suspensions are described in detail elsewhere [16]. Briefly, the suspensions contained 10 vol% HA particles (average particle size < 1 μm; Alfa Aesar, Haverhill, MA), 0.75 wt% dispersant (Dynol 604; Air Products & Chemicals, Inc., Allentown, PA), and 1.5 wt% binder (DuPont Elvanol® 90-50; DuPont, Wilmington, DE). Aqueous suspensions, as well as suspensions containing 60 wt% dioxane (Fisher Scientific, St. Louis, MO), were prepared using the same method. A concentration of 60 wt% dioxane was used because it resulted in the preparation of HA scaffolds with larger pore width than the scaffolds prepared from aqueous suspensions. Unidirectional freezing was performed by pouring the suspensions into poly(vinyl chloride), PVC, tubes ($\sim$10 mm internal diameter $\times$ 20 mm long) placed on a cold steel substrate at -20°C in a freeze dryer (Genesis 25 SQ Freeze Dryer, VirTis Co., Gardiner, NY). After sublimation of the frozen solvent in the freeze dryer, the constructs were sintered in air, for 3 h at 1350°C (heating and cooling rate = 3°C/min). Scaffolds for cell culture experiments were prepared by sectioning the sintered constructs using a diamond-coated blade, washing three times with de-ionized water and ethanol, and drying at 100°C.

2.2 Cell culture

HA scaffolds (8 mm in diameter $\times$ 2 mm thick) were dry heat sterilized for 24 h at 500°C prior to cell culture. The established MC3T3-E1 line of mouse pre-osteoblastic cells was obtained from ATCC and cultured in α-MEM medium supplemented with 10% fetal bovine serum plus 100 U/ml penicillin and 100 μg/ml streptomycin sulfate. The scaffolds were seeded with 60,000 MC3T3-E1 cells suspended in 100 μl of complete medium, and incubated for 4 h to permit cell attachment. The cell-seeded constructs were then transferred to a 24-well plate containing 2 ml of complete medium per well. The control group consisted of the same number of cells seeded in wells containing 2 ml of complete medium. All cultures were maintained at 37°C in a humidified atmosphere of 5% CO_2, with the medium changed every 2 days.

2.3 MTT staining of viable cells

Cell-seeded scaffolds (four from each group) were placed in 400 μl serum-free medium containing 100 μg of the tetrazolium salt MTT for the last 4 h of incubation to permit visualization of metabolically active cells on and within the porous HA constructs. After the incubation, the constructs were briefly rinsed in PBS and blotted dry. Images of the constructs were obtained using a stereomicroscope fitted with a digital camera to qualitatively assess the distribution of insoluble purple formazan, a product of mitochondrial reduction of MTT by viable cells. The MTT-labeled constructs were then frozen at -70°C, and fractured with a cooled microtome blade, and the fracture cross-section was visually examined to assess the presence of purple formazan within the interior of the constructs. Finally, the formazan product was extracted from the HA constructs with 1.0 ml ethanol and measured spectrophotometrically at 550 nm in a BMG FLUORstar Optima plate reader.

2.4 Cell morphology

At culture intervals of 2, 4 and 6 days, HA scaffolds with attached cells were removed, washed twice with warm PBS, and soaked overnight in 2.5% glutaraldehyde in PBS. The fixed samples were then washed with PBS three times,

dehydrated with a graded ethyl alcohol series, and soaked for 10 min in hexamethyldisilazane (HMDS). After a second soak in HMDS, the samples were allowed to dry in air for 12 h at room temperature for the liquid to fully evaporate, sputter-coated for 60 s with Au/Pd, and observed in a scanning electron microscope, SEM (Hitachi S-4700), at 5 kV accelerating voltage.

2.5 Quantitative protein assay

Total protein in lysates recovered from the cell-seeded scaffolds was measured to assess cell proliferation on the scaffolds. The scaffolds were placed in 500 µl of 1% Triton X-100 and the cells lysed by two freeze-thaw cycles (−80/37°C). Aliquots of the released lysate were mixed with a working reagent prepared from a micro-BCA Protein Assay Kit (Piece Biotechnology, Rockford, IL) and incubated at 50°C for 20 min. Sample absorbance values were measured at 550 nm in a BMG FLUORstar Optima plate reader with bovine serum albumin used as a standard for comparison.

2.6 Alkaline phosphatase activity

MC3T3-E1 cells were seeded onto HA constructs and plastic control wells with a density of 60,000 cells per scaffold or well. After culturing for 2, 4 and 6 days, the cell-seeded scaffolds were removed and washed twice with PBS. The samples were placed in 500 µl of 1% Triton X-100 and cells were lysed using two −80/37°C cycles. Aliquots of the lysate (120 µl) were placed in a 96-well plate for spectroscopic measurement of alkaline phosphate (ALP) using 0.5 M 2-amino-2-methyl-L-propanol (AMP) buffer containing 50 mM *p*-nitrophenyl phosphate (*p*-NPP) according to a previously described method [23]. ALP activity is expressed as nanomoles of *p*-NP released per min.

2.7 Statistical analysis

All biological experiments (four samples in each group) were run either in duplicate or triplicate. The data are presented as the mean ± standard deviation. Statistical analysis was performed using Student's *t*-test. Values were considered to be significantly different when $P < 0.05$.

3 Results and discussion

Table 1 summarizes the microstructural characteristics of the two groups of HA scaffolds used in the experiments. SEM images of the cross-sections perpendicular to the direction of freezing (Fig. 1a, b) showed no marked changes in the microstructure along the length of the sample, so each cross-section was, in general, representative of the whole construct. The two groups of scaffolds contained approximately the same total porosity (65–70%), but their microstructure and pore size (diameter or width) were different. Scaffolds prepared from aqueous suspensions had a lamellar-type microstructure (Fig. 1a), resulting from the hexagonal crystal structure of ice [24]. The inter-lamellar pores were 100–250 µm long and 25 ± 5 µm wide in cross section. Addition of dioxane to the aqueous suspension produced drastic changes in the microstructure, resulting from phase separation of the binary water–dioxane mixture during freezing and modification of the hydrogen bonding of water by the polar dioxane molecules [24]. Scaffolds prepared from suspensions with 60 wt% dioxane had a cellular-type microstructure, approximately cylindrical pores, and pore diameters of size 100 ± 10 µm (Fig. 1b).

We were unable to prepare cellular- and lamellar-type scaffolds with comparable pore diameters (or widths). Freezing of aqueous suspensions of ceramic particles typically leads to the production of scaffolds with narrow lamellar-type pores (typically <40 µm wide) [14–18]. The primary objective of the present work was to evaluate the in vitro cell culture response to scaffolds with the cellular-type microstructure because these scaffolds had the requisite porosity and pore size reported for scaffolds capable of supporting cell proliferation and function [19, 20]. Scaffolds with the lamellar-type microstructure were evaluated for comparison because they were reported to have high strength and potential for bone repair applications despite their narrow pore widths [14, 15].

SEM images in Fig. 1a–f show the morphology of MC3T3-E1 cells after 2, 4, and 6 days of culture on the scaffolds with the lamellar- and cellular-type microstructures. Cells grown on the lamellar constructs were elongated and appeared to align along the walls of the construct at low cell density after culturing for 2 and 4 days (Fig. 1a, c). A high magnification image (Fig. 1a, inset) shows the formation of numerous cell projections along the

Table 1 Microstructural characteristics of HA scaffolds prepared by unidirectional freezing of suspensions (10 vol% particles) and used in this work

Solvent composition	Microstructure	Pore width (µm)	Porosity (%)
Water	Lamellar	25 ± 5	70 ± 5
Water + dioxane (60 wt%)	Cellular	100 ± 10	65 ± 2

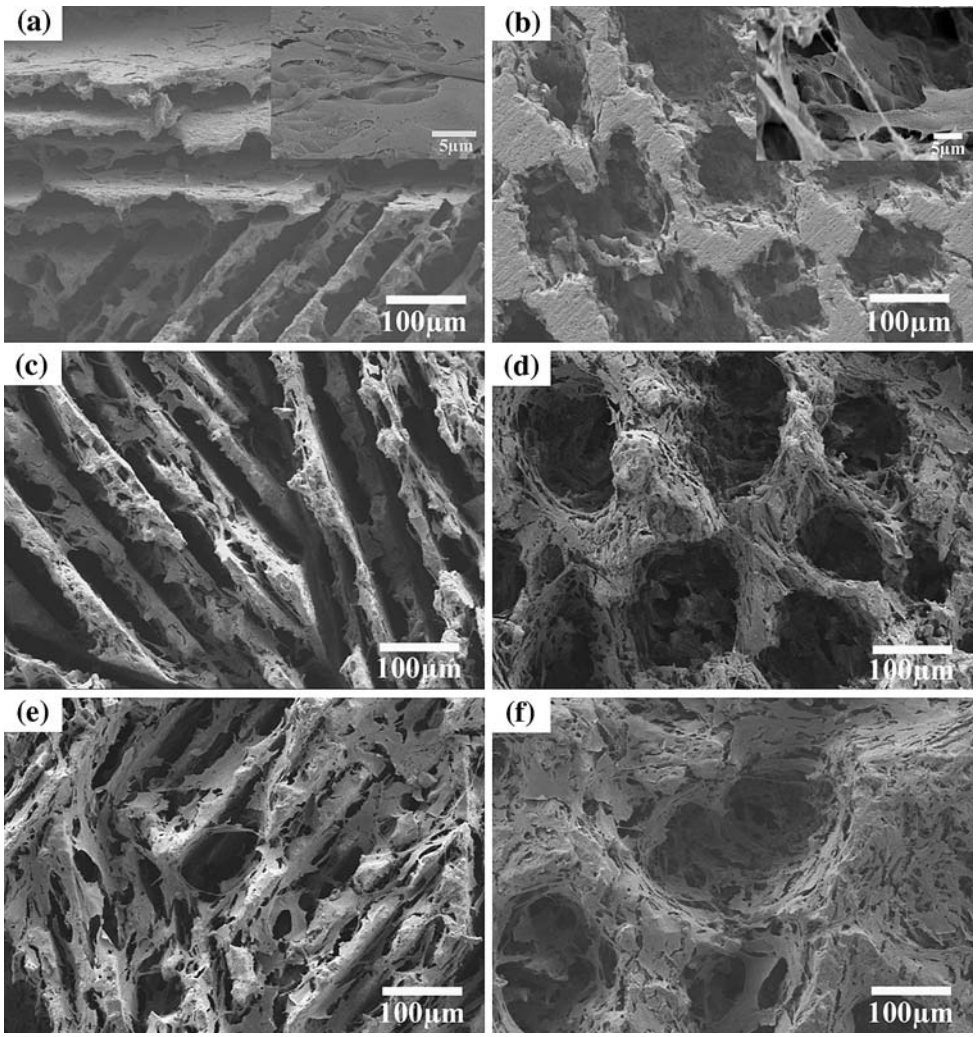

Fig. 1 SEM images of MC3T3-E1 cell morphology on freeze-cast constructs with **a**, **c**, **e** lamellar-type and **b**, **d**, **f** cellular-type microstructures after culturing for **a**, **b** 2 days; **c**, **d** 4 days; **e**, **f** 6 days

walls of the lamellae, features that indicated firm cell attachment to the surface. After culturing for 6 days (Fig. 1e), the cell number increased, and the cells bridged the lamellae and covered the surface of the constructs. After 2 and 4 days, the morphology of cells grown on the cellular constructs was generally similar to that observed on lamellar constructs. The cells were attached to the constructs with cell projections at day 2 interval (Fig. 1b, and inset). The cell density increased with culture time and, after 4 days, the cells colonized the surface of the constructs (Fig. 1d). After 6 days, the surface was almost completely covered with cells (Fig. 1f). However, instead of bridging the pores and concentrating on the surface as observed for the lamellar constructs (Fig. 1e), the cells apparently grew along the pore walls of the cellular constructs and were observed down into the pores. The cells were aggregated, and appeared to maintain physical contact with each other by multiple extensions with neighboring cells.

Results of the quantitative assay of total protein in cell lysates recovered from the HA constructs with the lamellar and cellular microstructures and from the control wells after incubations for 2, 4, and 6 days are shown in Fig. 2. The amounts of protein recovered from both types of scaffolds showed a nearly linear increase in cell proliferation during the 6-day incubation, a finding that complemented the progressive increase in cell density seen in the SEM images. The cell proliferation kinetics on the HA constructs were faster than on the control wells. Furthermore, cell proliferation on the cellular constructs was higher than on the lamellar constructs.

Photographic images of cell-seeded scaffolds treated with MTT during the last 4 h of incubation are shown in Fig. 3. The purple pigment visible on the scaffold was the result of mitochondrial reduction of MTT to an insoluble formazan product, an indication of viable cells. The increase in intensity of the purple color on the surface of both types of constructs with culture time indicated the proliferation of viable, metabolically active cells on the scaffolds (Fig. 3a, c). The relative amount of purple formazan visible on the freeze-fracture face of the scaffolds cultured for 6 days

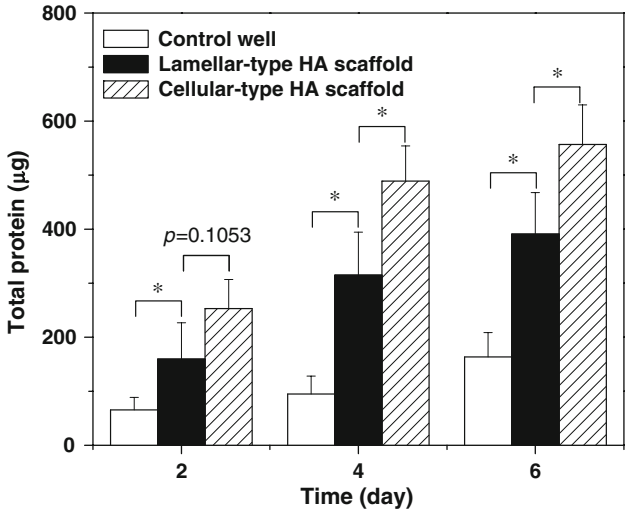

Fig. 2 Quantitative measurement of total protein content of cell-seeded scaffolds or control incubated for 2, 4, and 6 days. Mean ± SD; $n = 4$. *Significant increase in total amount of protein on the porous HA constructs with increasing culture duration ($P < 0.05$)

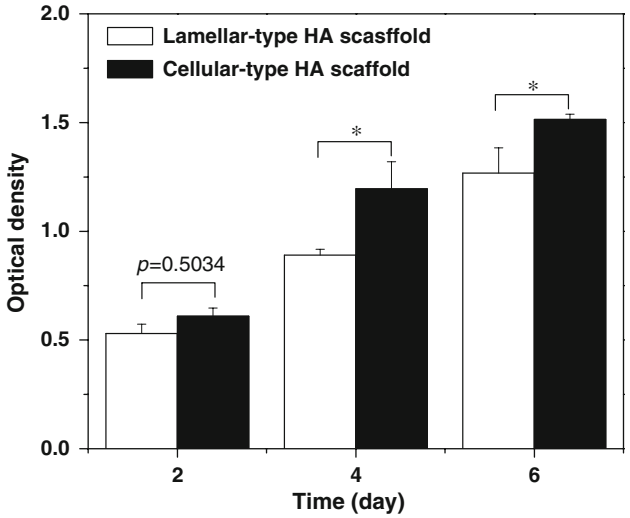

Fig. 4 Quantitative analysis of the purple formazan on the HA constructs with lamellar- and cellular-type microstructures. Mean ± SD; $n = 4$. *Significant increase in formazan extracted from the porous HA constructs with increasing culture duration ($P < 0.05$)

indicated that most of the metabolically active cells were predominantly near the surface of the lamellar construct (Fig. 3b). On the other hand, purple formazan covered a larger area of the freeze-facture surface and extended almost halfway into the interior of the cellular construct, indicating far higher cell proliferation into the interior.

Figure 4 shows results of spectrophotometric measurement of the amount of the formazan extracted from the constructs described in Fig. 3. The optical density (OD) value of the extraction was an indication of the amount of formazan and hence the viable cells in the constructs. The higher OD value indicated a larger amount of viable cells. The data showed that HA constructs with the cellular microstructure had larger OD values than the lamellar constructs at day 4 and 6, indicating that the cellular constructs had a better ability to support cell growth, a finding complemented by the higher amount of protein measured in the cellular constructs than the lamellar ones.

Results of spectrophotometric measurement of alkaline phosphatase activity of MC3T3-E1 cells cultured on the HA constructs for 2, 4 and 6 days are presented in Fig. 5. The alkaline phosphatase activity increased with the duration of incubation. This finding is an indication that the seeded cells were able to function as osteoblasts on the HA constructs. The higher alkaline phosphatase activity of the HA constructs with the cellular microstructure indicated that these constructs were better able to support cell function than the lamellar constructs.

In addition to being bioactive and providing adequate mechanical strength, scaffolds intended for the repair of

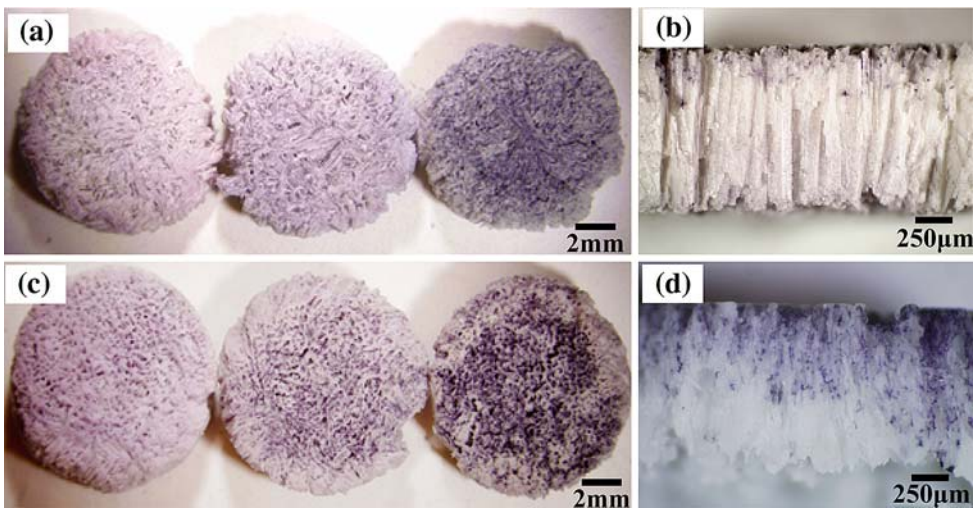

Fig. 3 Cell-seeded HA constructs treated with MTT: (*left*) surface of constructs with **a** lamellar-type and **c** cellular-type microstructure after culture intervals of 2, 4, and 6 days (left to right, respectively); (*right*) freeze-fracture section of scaffold cultured for 6 days, showing considerably greater infiltration of MTT-labeled cells into the interior of the cellular microstructure **d** than in the lamellar microstructure **b**

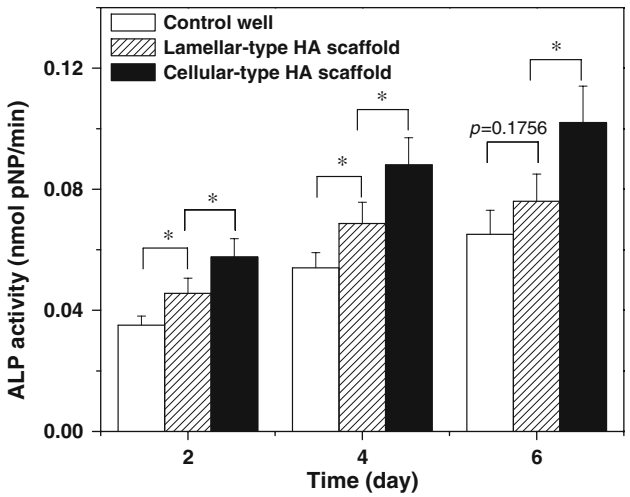

Fig. 5 Alkaline phosphatase activity of MC3T3-E1 cells cultured on two types of freeze-cast HA scaffolds (lamellar- and cellular-type) and control wells. Enzyme activity is expressed as nmol of *p*-NP formed per min. Mean ± SD; $n = 4$. *Significant increase in enzyme activity on the porous HA constructs with increasing culture duration ($P < 0.05$)

large defects in load-bearing bones should also support the ingrowth of cells and new tissues. Oriented bioceramic microstructures prepared by unidirectional freezing of aqueous suspensions have shown the ability to develop higher strength in the orientation direction, when compared to more random microstructures prepared by conventional freezing and other methods [14–18]. However, scaffolds prepared by unidirectional freezing of aqueous suspensions typically have a lamellar-type microstructure with narrow slot-like pores (width = 10–40 μm). The results of the present work showed that these lamellar-type scaffolds have limited ability to support cell infiltration and, therefore, the ingrowth of new tissues.

Scaffolds with the cellular-type microstructure (pore width = 100 ± 10 μm), prepared from HA suspensions with dioxane (60 wt%), not only had better ability to support the proliferation and function of MC3T3-E1 cells but also supported the proliferation of the cells down the porosity into the interior of the scaffolds. This coupled with the ability of the scaffolds to develop high compressive strength and large strain for failure shown in our previous work [16–18] indicates that these freeze-cast scaffolds may have potential applications in bone repair. Additional work is presently underway to evaluate the performance of these scaffolds for use in the repair of large defects in load-bearing bones in vivo.

4 Conclusions

The ability of two groups of hydroxyapatite (HA) scaffolds with different oriented pore architectures to support the proliferation and function of MC3T3-E1 pre-osteoblastic cells in vitro was evaluated. While both groups of scaffolds supported greater cell proliferation and differentiation when compared to control wells, scaffolds with the cellular-type microstructure (pore diameter = 100 ± 10 μm) showed better ability to support cell proliferation and function than lamellar-type scaffolds with slot-like pores of width 25 ± 5 μm. Cells proliferated predominantly on the surface of the lamellar scaffolds with little growth into the pores. On the other hand, cells proliferated both on the surfaces as well as deeper into the interior of the pores for the cellular microstructure. HA scaffolds with the oriented, cellular microstructure should have potential applications as biological scaffolds for bone repair and regeneration.

References

1. L.L. Hench, Bioceramics. J. Am. Ceram. Soc. **81**, 1705–1728 (1998)
2. A. El-Ghannam, Bone reconstruction: from bioceramics to tissue engineering. Expert Rev. Med. Devices **2**, 87–101 (2005). doi:10.1586/17434440.2.1.87
3. M.N. Rahaman, R.F. Brown, B.S. Bal, D.E. Day, Bioactive glasses for non-bearing applications in total joint replacement. Semin. Arthroplasty **17**, 102–112 (2006). doi:10.1053/j.sart.2006.09.003
4. L.M. Rodríguez-Lorenzo, M. Vallet-Regí, J.M.F. Ferreira, Fabrication of porous hydroxyapatite bodies by a new direct consolidation method: starch consolidation. J. Biomed. Mater. Res. **60**, 232–240 (2002). doi:10.1002/jbm.10036
5. S.H. Li, J.R. De Wijn, P. Layrolle, K. De Groot, Synthesis of macroporous hydroxyapatite scaffolds for bone tissue engineering. J. Biomed. Mater. Res. **61**, 109–120 (2002). doi:10.1002/jbm.10163
6. P. Sepulveda, J.G. Binner, S.O. Rogero, O.Z. Higa, J.C. Bressiani, Production of porous hydroxyapatite by the gel-casting of foams and cytotoxic evaluation. J. Biomed. Mater. Res. **50**, 27–34 (2000). doi:10.1002/(SICI)1097-4636(200004)50:1<27::AID-JBM5>3.0.CO;2-6
7. N. Tamai, A. Myoui, T. Tomita, T. Nakase, J. Tanaka, T. Ochi, H. Yoshikawa, Novel hydroxyapatite ceramics with an interconnective porous structure exhibit superior osteoconduction in vivo. J. Biomed. Mater. Res. **59**, 110–117 (2002). doi:10.1002/jbm.1222
8. Q.Z. Chen, I.D. Thompson, A.R. Boccaccini, 45S5 Bioglass®-derived glass-ceramic scaffold for bone tissue engineering. Biomaterials **27**, 2414–2425 (2006). doi:10.1016/j.biomaterials.2005.11.025
9. C. Wu, J. Chang, W. Zhai, S. Ni, J. Wang, Porous akermanite scaffolds for bone tissue engineering: preparation, characterization, and in vitro studies. J. Biomed. Mater. Res. B Appl. Biomater. **78B**, 47–55 (2006). doi:10.1002/jbm.b.30456
10. Q. Fu, M.N. Rahaman, B.S. Bal, R.F. Brown, D.E. Day, Mechanical and in vitro performance of 13-93 bioactive glass scaffolds prepared by a polymer foam replication technique. Acta Biomater. **4**, 1854–1864 (2008). doi:10.1016/j.actbio.2008.04.019
11. Q. Fu, M.N. Rahaman, W. Huang, D.E. Day, B.S. Bal, Preparation and bioactive characteristics of a porous 13-93 glass, and its fabrication into the articulating surface of a proximal tibia.

J. Biomed. Mater. Res. A **82A**, 222–229 (2007). doi:10.1002/jbm.a.31156
12. J.G. Dellinger, J. Cesarano III, R.D. Jamison, Robotic deposition of model hydroxyapatite scaffolds with multiple architectures and multiscale porosity for bone tissue engineering. J. Biomed. Mater. Res. A **82A**, 383–394 (2007). doi:10.1002/jbm.a.31072
13. C.Y. Lin, T. Wirtz, F. LaMarca, S.J. Hollister, Structural and mechanical evaluations of a topology optimized titanium interbody fusion cage fabricated by selective laser melting process. J. Biomed. Mater. Res. A **83A**, 272–279 (2007). doi:10.1002/jbm.a.31231
14. S. Deville, E. Saiz, A. Tomsia, Freeze casting of hydroxyapatite scaffolds for bone tissue engineering. Biomaterials **27**, 5480–5489 (2006). doi:10.1016/j.biomaterials.2006.06.028
15. S. Deville, E. Saiz, R.K. Nalla, A. Tomsia, Freezing as a path to build complex composites. Science **311**, 515–518 (2006). doi:10.1126/science.1120937
16. Q. Fu, M.N. Rahaman, F. Dogan, B.S. Bal, Freeze casting of porous hydroxyapatite scaffolds—I. Processing and general microstructure. J. Biomed. Mater. Res. B Appl. Biomater. **86B**, 125–135 (2008). doi:10.1002/jbm.b.30997
17. Q. Fu, M.N. Rahaman, F. Dogan, B.S. Bal, Freeze casting of porous hydroxyapatite scaffolds—II. Sintering, microstructure, and mechanical properties. J. Biomed. Mater. Res. B Appl. Biomater. **86B**, 514–522 (2008). doi:10.1002/jbm.b.31051
18. Q. Fu, M.N. Rahaman, F. Dogan, B.S. Bal, Freeze-cast hydroxyapatite scaffolds for bone tissue engineering applications. Biomed Mater **3**, 025005 (2008). doi:10.1088/1748-6041/3/2/025005
19. J.O. Hollinger, K. Leong, Poly(a-hydroxy acids): carriers for bone morphogenetic proteins. Biomaterials **17**, 187–194 (1996). doi:10.1016/0142-9612(96)85763-2
20. Y.H. Hu, D.W. Grainger, S.R. Winn, J.O. Hollinger, Fabrication of poly(a-hydroxy acid) foam scaffolds using multiple solvent systems. J. Biomed. Mater. Res. **59**, 563–572 (2002). doi:10.1002/jbm.1269
21. S. Foppiano, S.J. Marshall, G.W. Marshall, E. Saiz, A.P. Tomsia, The influence of novel bioactive glasses on in vitro osteoblast behavior. J. Biomed. Mater. Res. A **71A**, 242–249 (2004). doi:10.1002/jbm.a.30159
22. R.F. Brown, D.E. Day, T.E. Day, S. Jung, M.N. Rahaman, Q. Fu, Growth and differentiation of osteoblastic cells on 13-93 bioactive glass fibers and scaffolds. Acta Biomater. **4**, 387–396 (2008). doi:10.1016/j.actbio.2007.07.006
23. A. Sabokar, P.J. Millett, B. Myer, N. Rushton, A rapid, quantitative assay for measuring alkaline phosphatase in osteoblastic cells in vitro. Bone Miner. **27**, 57–67 (1994). doi:10.1016/S0169-6009(08)80187-0
24. M.N. Rahaman, Q. Fu, Manipulation of porous bioceramic microstructures by freezing of aqueous suspensions with binary mixtures of solvents. J. Am. Ceram. Soc. **91**(12), 4137–4140 (2008). doi:10.1111/j.1551-2916.2008.02795.x